

Spectral-Based Six-Color Separation Minimizing Metamerism

Di-Yuan Tzeng
Applied Science Fiction, Inc.
Austin, Texas

Roy S. Berns
Munsell Color Science Laboratory
RIT Chester F. Carlson Center for Imaging Science
Rochester, New York

Abstract

A spectral-based six-color printer model was derived in determining the six color separations for an input spectral image that yields the least metameric reproduction relative to the original. Confined by the ink-trapping limitation, the six-color halftone printer modeling effort is a union of ten four-color halftone printer modeling efforts in addition to a four-ink selector. The four-ink selector defines a set of the best four inks providing the closest spectral fit to an input pixel requiring reproduction in a continuous tone approximated space. Then the four-ink backward halftone printer model corresponding to the selected ink set for an input pixel calculates the ink amount in terms of fractional dot areas for synthesizing the pixel. This completes the proposed spectral six-color separation algorithm.

This article will discuss the construction of the four-ink selector, approaches on dividing the six-color printer model into ten four-color printer models, performance in terms of colorimetric and spectral accuracy of the model, and, finally, the colorimetric and spectral performance comparison between the proposed six-color and conventional four-color printer models.

Introduction

Metamerism between original objects and their corresponding reproductions can be minimized by utilizing a multi-spectral imaging system. A multi-spectral imaging system is comprised of multi-spectral acquisition[1-7] and spectral-based printing.[8-11] This is one of the focused and ongoing research activities in the Munsell Color Science Laboratory of Rochester Institute of Technology.[12]

The responsibility of the current authors was to develop spectral-based printing algorithms limited at using one black and five chromatic inks as the output module for an end-to-end multi-spectral imaging system. This output module contained five subsystems: colorant estimation, ink selection algorithm, ink overprint prediction, spectral-based color separation minimizing metamerism, and multi-ink printing, diagramed in Figure 1.

The research contents of the colorant estimation and ink selection algorithm were published and presented in Color Imaging Conference 1998 and 1999, respectively.[13-14] The research effort of ink overprint prediction was presented in the TAGA/ISCC Symposium, Vancouver 1999.[15] The current submission is to describe the technical strategies in building a set of six color separation algorithms minimizing metamerism.

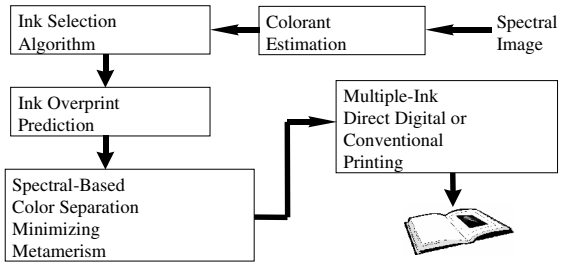

Figure 1: The proposed spectral-based output system minimizing metamerism.

Conventional four-color printing is limited by insufficient degrees of freedom. It achieves, at best, a metameric reproduction. The utilization of two more inks increases the color gamut and the number of degrees of freedom. Therefore, it enhances the possibility of colorimetric and spectral matching. Most multi-ink printing systems whose color separation algorithms are focused on trichromatic matching do not take advantage of more degrees of freedom. The resultant color reproduction still suffers unstable color matching due to an uncontrollable viewing environment. Hence, this research was aimed at

minimizing metamerism by deriving six-color separation algorithms that achieve close spectral reproductions.

The proposed six-color separation algorithms were derived based on existing spectral-based four-color separation algorithms published by Iino and Berns.[8-10] This research project subdivided a six-color halftone printer modeling effort into ten four-color halftone printer modeling efforts. As a result, the proposed spectral six-color printer model was a union of ten four-color spectral halftone printer models.

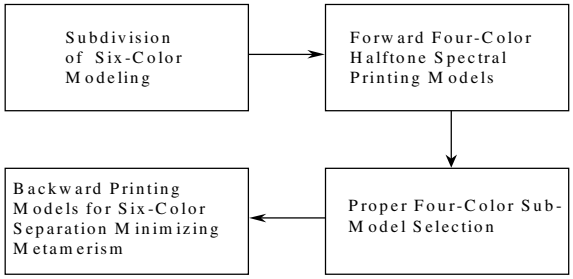

Figure 2: The proposed process flow of the spectral-based six-color printer models for color separation.

There is a physical limitation that the total amount of inks in a pixel printed with more than 400% dot area coverage will most likely collapse. This is a well-known phenomenon called the ink-trapping limitation. Hence, it is not practical to print all six inks together on a pixel. Furthermore, if a pixel needs six inks to be synthesized, then its spectrum can be approximated by a set of four carefully chosen inks. Hence, our ink-limiting scheme is to dynamically select one black and three chromatic inks from the six printer primaries to synthesize a pixel to avoid ink-trapping failure. There are ten combinations of choosing three out of the five chromatic inks since the black ink was a fixed choice. Therefore, our forward six-color printer model is a collection of ten forward four-primary printer models. Based on these predefined constraints, the proposed backward six-color printer model requires a four-ink selector to determine a subset of four inks giving the best spectral fit for an input pixel requiring reproduction. The backward printer model solves the ink amount in terms of fractional dot areas required to deliver on a paper substrate. This completes the development of the spectral-based six-color separation.

Theoretical Background

Since the proposed six-color printer model is the union of ten four-color printer models, it is sufficient to only discuss the halftone color formation of the four-color case. The analytical description for the halftone color formation is based on the Yule-Nielsen modified spectral Neugebauer equation,[16] show as Eq. (1),

$$R_\lambda = [\sum_{i=1}^{16} a_i R_{\lambda,i}^{1/n}]^n , \qquad (1)$$

where R is the reflectance factor, λ represents the visible wavelength, a is the fractional dot area for synthesizing a spectrum, and n is the Yule-Nielsen dot-gain factor. Notice that the $R_{\lambda,i}$ represents the spectral reflectance factor of a so-called Neugebauer primary and its associated effective dot area, a_i, is a function, which is described by the Demichel equation,[17] of the probable occurrence of the four primary inks, e.g., cmyk, that are used for a halftone printing process. Equation (1) can be analytically solved for the effective dot areas, a_i, for each Neugebauer primary followed by numerically solving for the required ink amount (or termed as theoretical dot area) for each primary to be delivered on a paper substrate. The model training process is completed by first making samples (mostly ramps) with known theoretical dot areas (or termed requested dot areas), second, solving Eq. (1) for the corresponding effective dot areas, and finally, relating the theoretical to the effective dot areas. The printer model determined by this straightforward approach is termed as the first order printer model.

Occasionally, the first order approach provides good enough colorimetric and spectral accuracy. However, the usual case is that the optical interaction among ink layers often causes first order approach to be ineffective. The first order approach frequently over-predicts the effective ink amount in terms of fractional dot area, as a consequence, it under-predicts the spectral reflectance factor. Experiential evidence and previous research had shown that the optical interaction among ink layers actually yields smaller effective dot area.[8-10] Iino and Berns proposed a second order approach to account for the optical interaction. The basic idea is that the dot-gain of a primary ink is a function of the existence of the other primary inks. When no other primary ink coexists on a pixel, the dot-gain of a primary ink printed on a paper substrate is at its maximum. Dot-gain is attenuated by increasing the amount of the other primary ink appearing at the same pixel location. Iino and Berns generated samples for empirically modeling the optical interaction among ink layers by printing a primary ramp on top of the other primary ink with uniform ink coverage. The ratio between the dot-gain curve of a primary ink printed with and without a second coexisting ink is the dot-gain attenuation which modifies the effective dot area, a_i, in Eq. (1). They repeated this process using the different ink coverage of the second coexisting primary to determine the dot-gain attenuation function. The second-order modification dramatically improves the model accuracy.

The proposed six-color separation algorithm is based on Iino and Berns' approach to construct ten four-color forward halftone printer models. Once a forward printing model with the highest performance in terms of colorimetric and spectral accuracy is adopted, the task of color separation is to invert this forward printer model and solve for the ink amount required for the best spectral fit of an input pixel. Due to the high nonlinearity of halftone printer

models, numerical inversion was utilized to complete the backward modeling.

The spectral-based six-color backward printer model proposed by this research and diagrammed in Figure 3 comprises a four-ink selector, ten spectral-based four-color forward printing models, and a constrained optimization engine.

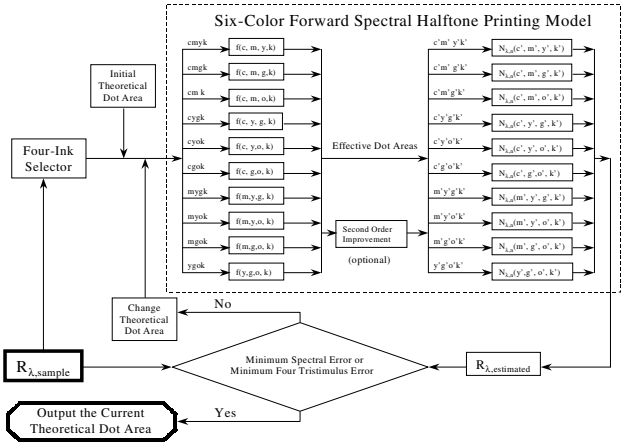

Figure 3: The structure chart of the proposed six-color backward spectral printer model.

In Figure 3, those components inside the dashed box constitute the proposed six-color forward spectral halftone printer model, which is comprised of ten forward four-color models. Each four-color model contains a function that relates the theoretical dot areas, denoted as cmyk for example, to the effective dot areas, denoted as c'y'm'k', solved by Eq. (1) at the model training stage. Then the effective dot areas are input to the Yule-Nielsen modified spectral Neugebauer equation for estimating a spectrum.

Outside the dashed box, the remainder process is completed by a numerical optimization engine. The process of the spectral-based six-color separation starts from a given reflectance spectrum depicted as an input module located at the lower left corner. The four inks most likely to reproduce an input spectrum are determined by a four-ink selector. This selector is implemented using continuous tone approximation such that the candidate set is a set of one black and three chromatic inks selected from the six primary inks whose linear combination in a linear colorant mixing space is the best spectral fit of an input spectrum. The continuous tone approximation is based on the Kubelka-Munk transformation for transparent material in optical contact with an opaque substrate such as paper.[18] The transformation to determine the spectral absorption coefficient, K, of a transparent ink is described by Eq. (2),

$$K_{\lambda,ink} = -0.5 \cdot X^{-1} \cdot \ln(R_{\lambda,ink} / R_{\lambda,g}), \qquad (2)$$

where λ is a visible wavelength, X is the thickness of an ink layer, $R_{\lambda,ink}$ is the spectral reflectance factor of an ink, and $R_{\lambda,g}$ is the spectral reflectance factor of a substrate. The spectral fit of a pixel requiring reproduction in absorption space is a linear combination of the absorption spectra of the four-primary inks, shown as Eq. (3),

$$K_{\lambda,pixel} = \sum_{i=1}^{4} c_i \cdot K_{\lambda,ink\_i}, \qquad (3)$$

where c represents the concentration of an ink. The four-ink selector will choose the set whose error is the minimum among the ten sets for every pixel of an input spectral image.

Once the ink set is selected for an input pixel, the optimization engine initializes a set of theoretical dot areas, which are approximated by the concentrations estimated in the linear color mixing space, corresponding to the selected four inks. The forward printer model then estimates the spectrum located at the lower right corner of the diagram. The decision module in the diamond-shaped box located in the lower center compares the input and output spectra at this iteration stage. If the spectral reconstruction satisfies the error criteria then the set of theoretical dot areas at this stage is output and the iteration terminated. If not, the next module modifies the set of theoretical dot areas for the next iteration.

Initially, the optimization criterion was to minimize the spectral error. If the spectral minimization yielded unsatisfactory accuracy, then the optimization pursues balancing spectral and colorimetric accuracy. Because the six-color forward spectral printing model is composed of ten forward four-color sub-models, the optimization criteria for balancing spectral and colorimetric accuracy could be achieved by minimizing the total error of "four tristimulus values." The first three tristimulus values are obtained by the tristimulus values under the standard viewing illumant, e.g., D50 for printing industry. The fourth value is the tristimulus X calculated under second standard viewing illumant such as A, based on the research by Allen.[19]

Experimental

In order to verify the proposed algorithm in building a six-color spectral halftone printing model, the current research utilized the DuPont WaterProof® system to represent a halftone printing process. The standard cyan (C), magenta (M), yellow (Y), black (K), green (G), and orange (O) designed for the DuPont WaterProof® system were recommended for use as the six printing primaries for a stable proofing process. The spectral reflectance factors of the printed six primaries and the paper substrate (100# Vintage Gloss Text) are plotted in Figure 4.

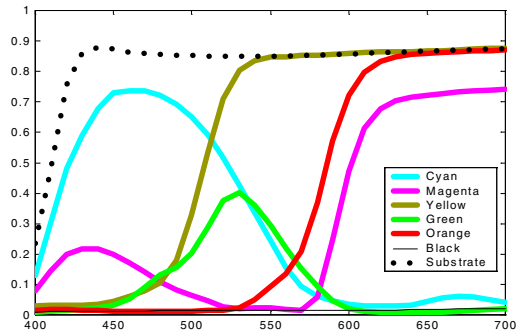

Figure 4: The reflectance spectra of the printed six primaries and substrate.

Usually, modeling of the halftone printing process requires a set of ramps including primary, secondary, tertiary, quaternary, etc., in addition to a verification target representing a device gamut. Since this research aims at developing a six-color printing system, the preparation for each printed sample patch utilized FM screening to avoid moiré patterns. The screen frequency was chosen at 175 LPI resolution or equivalent to account for the most common and practical conditions. The following is the list of the sample and target specifications for the proposed six-color printer modeling process.

Preparation for Ramps

Each ramp was printed at 5%, 10%, 15%, 20%, 30%, 40%, 50%, 60%, 70%, 80%, 90%, and 100% of theoretical dot areas. For a four-color halftone printing process, there are secondary (two-ink overprints), tertiary (three-ink overprints), and quaternary (four-ink overprints). Although this research used six primary inks for halftone reproduction, the approach to reproduce an input color (spectrally) is limited to use one black and three chromatic inks for synthesis. Therefore, five-ink and six-ink overprints are not generated in the six-color printing process. The overprints are categorized by the number of inks and listed as follows. There were fifteen two-ink overprint combinations (C(6,2)) selecting two inks out of six. They were CM, CY, CG, CO, CK, MY, MG, MO, MK, YG, YO, YK, GO, GK, and OK. There were twenty three-ink overprint combinations (C(6,3)) selecting three inks out of six. They were CMY, CMG, CMO, CMK, CYG, CYO, CYK, CGO, CGK, COK, MYG, MYO, MYK, MGO, MGK, MOK, YGO, YGK, YOK, and GOK. There were ten four-ink overprint combinations (C(5,3)) selecting three chromatic inks out of five plus one black due to the constraint mentioned previously. They are CMYK, CMGK, CMOK, CYGK, CYOK, CGOK, MYGK, MYOK, MGOK, and YGOK.

Preparation of the Verification Target (5x5x5x5 Combinatorial Design For Mixtures)

Again, the constraint is to use black and three chromatic inks to reproduce each pixel from a spectral image. The six-color halftone printer model can be viewed as a superset of several sets of four-color halftone models. In this case, there were ten subsets of four-color halftone models. They are CMYK, CMGK, CMOK, CYGK, CYOK, CGOK, MYGK, MYOK, MGOK, and YGOK. There were 625 combinations for each subset, the 5x5x5x5 combinatorial design of mixtures modulated by five different fractional dot areas. To print the 625 mixtures for the CMYK sub-model, first twenty-five samples were printed on paper by varying the theoretical dot areas of cyan and magenta inks at the 0% of yellow and 0% of black ink. Then this printing procedure was repeated 25 times with yellow and black inks varying at five different fractional dot areas (0%, 25%, 50%, 70%, and 90%). Since there are ten sets of four-ink combinations in the proposed six-color model, the total number of samples was 6,250 for the 5x5x5x5 combinatorial design.

Sample Measurements

Samples were measured using a Gretag Spectrolino, whose sampling geometry is 0/45, with an automatic station to obtain reflectance spectra. The adopted spectral range was from 400 nm to 700 nm at 10 nm intervals. The spectral data of the ramps (total 612 patches) were obtained by averaging four measurements on each patch. Due to the large number of patches in the verification target (total 6,250), the spectral data of each of these patches were only measured once.

Accuracy Metric

The colorimetric accuracy was specified by the CIE94[20] color difference equation for standard illuminant D50 and the 1931 standard observer. The spectral accuracy was specified by a metamerism index which was quantified by the CIE94 color difference equation for standard illuminant A and the 1931 standard observer after a parameric correction.[21]

Spectral-Based Six-Color Separation for 171 Reflectance Spectra

A set of 171 reflectance spectra, which includes measurements of 63 flowers, 13 leaves, 52 man-made paints, 17 skin tones, and 26 spectra which are mostly rocks and dirt of natural vegetation was utilized to represent typical spectral information of a scene. Both the proposed six-color and conventional four-color technologies were utilized to color separate the 171 spectra for the performance comparison.

Results and Discussions

The second-order approach was employed for both the proposed six-color (using CMYKGO) and four-color (using CMYK) forward spectral printer models for the desired

model accuracy. The colorimetric and spectral accuracy for both models are shown in Table I, and the colorimetric and spectral accuracy of the reproduced 171 spectra using the proposed six-color and four-color models are shown in Table II, where RMS stands for the root-mean-square error of spectral reflectance factor.

Table I: The colorimetric and spectral accuracy for the spectral six-color and four-color second order forward printer models.

	Six-color		Four-Color	
	ΔE^*_{94}	M.I.	ΔE^*_{94}	M.I.
Mean	0.90	0.10	0.62	0.07
Stdev	0.75	0.10	0.43	0.08
Max	6.06	1.19	2.88	0.72
Min	0.00	0.00	0.04	0.00
RMS	0.004		0.003	

Table II: The colorimeric and spectral accuracy for the reproduced 171 spectra using the proposed six-color and four-color models.

	Six-color		Four-Color	
	ΔE^*_{94}	M.I.	ΔE^*_{94}	M.I.
Mean	1.16	0.67	1.38	1.05
Stdev	1.94	0.57	1.96	0.74
Max	10.48	3.09	11.04	3.79
Min	0.00	0.06	0.00	0.08
RMS	0.063		0.067	

Notice that the number of samples of the verification target is 6,250 for the six-color case and 625 for the four-color case since the verification target of the six-color case is the superset of the four-color case. Table I serves the purpose of showing that the second order approach provides the desired performance by their low colorimetric and spectral errors. Table II reveals that the backward printer model is capable of color separating the 171 spectra representing a typical scene using both the six-color and four-color models to achieve a satisfactory colorimetric accuracy.

The student *t*-test was utilized to test the mean difference of the colorimetric error produced by the six-color and four-color models in units of ΔE^*_{94}. It showed no significant difference. This means that the four-color technology has equal colorimetric performance to that of the proposed six-color technology. Nevertheless, the goal of the six-color approach is to minimize metamerism. Hence, attention was paid to the spectral performance between the two models. Again, the student *t*-test was used to test the mean difference between the two sets of metamerism indices produced by the six-color and four-color models. The result showed that the mean metamerism index of the six-color model was significantly lower than the mean of the four-color model. This means that the six-color technology reproduces the 171 spectra with higher spectral accuracy.

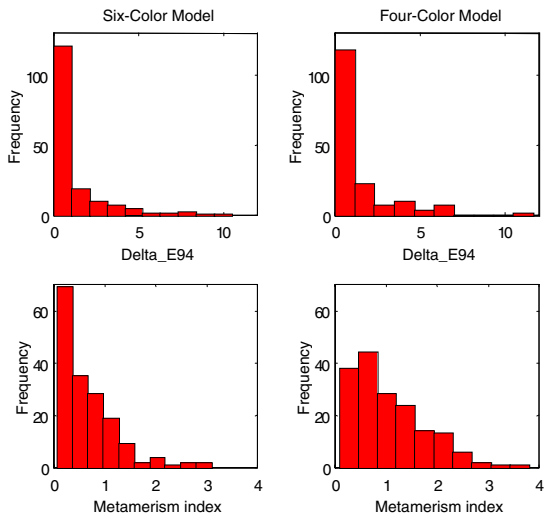

Figure 5: The histograms of the colorimetric error in unit of ΔE^*_{94} and the spectral error in units of metamerism index of the proposed six-color (left column) and four-color (right column) models.

Figure 5 shows the histograms of the colorimetric and spectral errors in units of ΔE^*_{94} and metamerism index, respectively, of the reproduced 171 spectra by the proposed six-color and the conventional four-color methods. It can be seen, that the histograms of the colorimetric error produced by the two technologies are visually similar (statistically the same by the student *t*-test). The histograms of the spectral errors produced by the two technologies are visually different for the larger number of spectra reproduced by the six-color approach with less than one unit of metamerism index. This confirms the statistical result of significantly better spectral performance. The data including the measured 171 spectra and their reproduced spectra by six- and four-color approaches, respectively, can be found at http://www.cis.rit.edu/~dxt1649/CIC2000/.

Conclusions

Spectral-based six-color separation algorithms were derived in building a six-color halftone printing system minimizing metamerism. The six-color modeling strategy is to be the union of ten four-color printer models together with a four-ink selector. The four-ink selector utilizes continuous tone approximation to determine the optimal ink set, which gives the best spectral fit of an input spectrum in absorption space. Spectral-based separation is completed by the backward spectral four-color printer model corresponding to the selected ink set calculating the ink amount in terms of theoretical dot area to be delivered on a paper substrate.

The proposed six-color spectral forward printer models is equipped with high colorimetric and spectral accuracy based on the Iino and Berns' optical interaction model. This provides a good basis for comparing the spectral performance between the proposed six-color and the

conventional four-color technology when a real world scene is encountered. By the comparison of overall accuracy between the proposed six-color and the conventional four-color technology using the 171 spectra representing a real world scene, colorimetric accuracy is about the same and, spectral performance is significantly enhanced by the proposed six-color separation algorithm. Hence, the degree of metamerism is significantly minimized.

Acknowledgment

The authors wish to express their thanks to E. I. du Pont de Nemours and Company, Inc., who financially supported this research.

References

1. P. D. Burns, Analysis of Image Noise in Multispectral Color Acquisition, Ph.D. Dissertation, Rochester Institute of Technology, 1997.
2. P. D. Burns and R. S. Berns, Error Propagation in Color Signal Transformations, Color Res. Appl. 22, 280-289 (1997).
3. P. D. Burns and R. S. Berns, Modeling Colorimetric Error in Electronic Image Acquisition, IS&T/OSA Optical Imaging in the Information Age, pg. 147-149. (1997).
4. P. D. Burns and R. S. Berns, Analysis of Multispectral Image Capture, Proc. 4th IS&T/SID Color Imaging Conference, pg. 19-22. (1996).
5. F. H. Imai and R. S. Berns, High-resolution multi-spectral image capture for fine arts preservation. Proc. 4th Argentina Color Conference, pg. 21-22. (1998).
6. F. H. Imai and R. S. Berns, High-resolution multi-spectral image archives: a hybrid approach, Proc. IS&T/SID 6th Color Imaging Conference, pg. 224-227. (1998).
7. F. H. Imai, R. S. Berns, and D. Y. Tzeng, A comparative analysis of spectral reflectance estimated in various spaces using a trichromatic camera system, J. Imag. Sci. Tech. 44 No. 4, 280-287 (2000).
8. K. Iino and R. S. Berns, A Spectral Based Model of Color Printing that Compensates for Optical Interactions of Multiple Inks, AIC Color 97, Proc. 8th Congress International Colour Association, pg. 610-613. (1997).
9. K. Iino and R. S. Berns, Building Color Management Modules Using Linear Optimization I. Desktop Color System, J. Imag. Sci. Tech. 42, 79-94 (1998).
10. K. Iino and R. S. Berns, Building Color Management Modules Using Linear Optimization II. Prepress System for Offset Printing, J. Imag. Sci. Tech. 42, 99-114 (1998).
11. D. Y. Tzeng, Spectral-Based Color Separation Algorithm Development for Multi-Ink Reproduction, Dissertation, Rochester Institute of Technology, 1999.
12. R. S. Berns, Challenges for Colour Science in Multimedia Imaging, in L. MacDonald and M. R. Luo, Eds., Colour Imaging: Vision and Technology, John Wiley & Sons, Chichester, 1999, pg. 99-127.
13. D. Y. Tzeng and R. S. Berns, Spectral-Based Ink Selection for Multiple-Ink Printing I. Colorants Estimation of Original Objects, Proc. 6th IS&T/SID Color Imaging Conference, pg. 106-111. (1998).
14. D. Y. Tzeng and R. S. Berns, Spectral-Based Ink Selection for Multiple-Ink Printing II. Optimal Ink Selection, Proc. 7th IS&T/SID Color Imaging Conference, pg. 182-187. (1999).
15. D. Y. Tzeng and R. S. Berns, Spectral Reflectance Prediction of Ink Overprints by Kubelka-Munk Turbid Media Theory, Proc. TAGA/ISCC Symposium in Vancouver B. C., pg. 682-697. (1999).
16. H. E. J., Neugebauer, Die Theoretischen Grundlagen des Mehrfarbenbuchdrucks, (German) Zeitschrift für Wissenshaftliche Photographie Photophysik und Photochemie 36:4, 73-89 (1937) [Reprinted in Proc. SPIE 1184: Neugebauer Memorial Seminar on Color Reproduction, 194-202 (1989).]
17. Demichel, M. E., Procédé 26, 17-21, 26-27 (1924).
18. P., Kubelka, and F. Munk, Ein Beitrag zur Optik der Farbanstriche, Z. Tech. Phys. (German) 12, 593-601 (1931).
19. Allen, E., Colorant Formation and Shading, in Optical Radiation Measurements, Volume 2, Color Measurement, F. Grum and C. J. Bartleson, Eds., Academic Press, New York, 1980, pg. 290-336.
20. CIE Technical Report 116, Industrial Color-Difference Evaluation, CIE, Vienna, 1995.
21. Fairman, Metameric Correction Using Parameric Decomposition, Color Res. Appl. 12, 261-265 (1987).

Biography

Dr. Di-Yuan Tzeng joined Applied Science Fiction as a color-imaging scientist since October 1999. He received his B.S. in Printing Technology from Chinese Culture University in Taipei, Taiwan, M.A. in Mathematics from Central Connecticut State University, and Ph.D. from the Munsell Color science Laboratory of Center for Imaging Science at Rochester Institute of Technology. His research topic for his dissertation is spectral-based color separation algorithm development for multiple-ink printing. He has also been a member of ISCC and IS&T since 1996 and a member of TAGA since 1999.